

Influence of the N/Z ratio on Disintegration Modes of Compound Nuclei

J.P. Wieleczo, E. Bonnet, J. Gomez del Campo, M. La Commara, J.D. Frankland, A. Chbihi, E. Rosato, G. Spadaccini, A. Galindo-Uribarri, D. Shapira, et al.

► **To cite this version:**

J.P. Wieleczo, E. Bonnet, J. Gomez del Campo, M. La Commara, J.D. Frankland, et al.. Influence of the N/Z ratio on Disintegration Modes of Compound Nuclei. FUSION08: New Aspects of Heavy Ion Collisions Near the Coulomb Barrier, Sep 2008, Chicago, United States. pp.64-69, 10.1063/1.3108862 . in2p3-00375772

HAL Id: in2p3-00375772

<http://hal.in2p3.fr/in2p3-00375772>

Submitted on 16 Apr 2009

HAL is a multi-disciplinary open access archive for the deposit and dissemination of scientific research documents, whether they are published or not. The documents may come from teaching and research institutions in France or abroad, or from public or private research centers.

L'archive ouverte pluridisciplinaire **HAL**, est destinée au dépôt et à la diffusion de documents scientifiques de niveau recherche, publiés ou non, émanant des établissements d'enseignement et de recherche français ou étrangers, des laboratoires publics ou privés.

Influence of the N/Z ratio on Disintegration Modes of Compound Nuclei

J.P. Wieleczko^a, E. Bonnet^a, J. Gomez del Campo^b, M. La Commara^c, M. Vigilante^c, J.D. Frankland^a, A. Chbihi^a, E. Rosato^c, G. Spadaccini^c, A. Galindo-Uribarri^b, D. Shapira^b, C.Beck^d, B. Borderie^e, R. Bougault^f, R. Dayras^g, G. De Angelis^h, P. Lantesseⁱ, N. Le Neindre^f, A. D'Onofrio^j, M. Parlog^f, D. Pierroutsakou^c, F. Rejmund^a, M.F. Rivet^e, M. Romoli^k and R. Roy^l

^aGANIL, CEA et IN2P3-CNRS, B.P. 55027, F-14076, Caen Cedex, France

^bPhysics Division, Oak Ridge National Laboratory, Oak Ridge, TN 37831, USA

^cDipartimento di Scienze Fisiche, Università di Napoli "Federico II", I 80126, Napoli, Italy

^dIPHC, IN2P3-CNRS, F 67037, Strasbourg Cedex2, France

^eIPNO, IN2P3-CNRS and Université Paris-Sud 11, F-91406, Orsay Cedex, France

^fLPC, IN2P3-CNRS, ENSICAEN and Université, F-14050, Caen Cedex, France

^gCEA, IRFU, SPhN, CEA/Saclay, F-91191, Gif sur Yvettes Cedex, France

^hINFN, LNL, I 35020 Legnaro (Padova) Italy

ⁱIPNL, IN2P3-CNRS et Université, F-69622, Villeurbanne Cedex, France

^jDipartimento di Scienze Ambientali, Università di Napoli, I 81100, Caserta, Italy

^kDipartimento di Scienze Fisiche, Università di Napoli "Federico II", I 81100, Caserta, Italy

^lLaboratoire de Physique Nucléaire, Université de Laval, Québec, Canada

Abstract. Investigations into the role of the N/Z ratio on the decay modes of compound nuclei are presented. Characteristics of fragments with atomic number $6 \leq Z \leq 28$ and light charged particles emitted in $^{78,82}\text{Kr} + ^{40}\text{Ca}$ at 5.5 MeV/A reactions were measured at the GANIL facility using the 4π -INDRA array. Data are compatible with an emission process from a compound nucleus. Persistence of structure effects and emission before full separation of fission fragments are evidenced from elemental cross-sections and coincidence data between light charged particles and fragments. Data are discussed in the framework of the transition state model.

Keywords: Fusion reactions; Light charged particles emission; Fission; Statistical models.

PACS: 24.10.Pa, 24.60.Dr, 25.70.Jj, 29.40.Wk

INTRODUCTION

The behaviour of nuclei produced under extreme conditions is of interest from both experimental and theoretical points of view. The fusion process between heavy ions colliding at incident energies around the Coulomb barrier is well-adapted to form compound nuclei in a controlled way in terms of excitation energy and angular momentum. These excited nuclei decay through a variety of channels and fundamental quantities, such as level density parameters, fission barriers or nuclear viscosity can be extracted from the study of these channels. The neutron enrichment (N/Z) of the compound nuclei is expected to play a role in the various emission mechanisms and nuclear quantities quoted above. In this contribution we present preliminary data on light charged particles and fragments emitted in $^{78,82}\text{Kr} + ^{40}\text{Ca}$ reactions at 5.5 MeV/A incident energy.

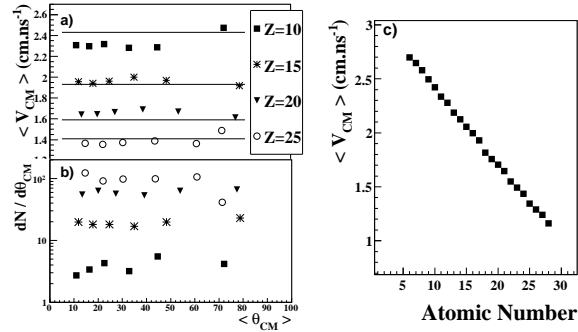


FIGURE 1. a) Experimental average velocity V_{cm} for fragments with atomic number $Z=10, 15, 20, 25$ emitted in the $^{78}\text{Kr}+^{40}\text{Ca}$ reaction as a function of the emission angle in the centre-of-mass; b) angular distribution for fragments with atomic number $Z=10, 15, 20, 25$ in the centre-of-mass; c) average centre-of-mass V_{cm} for fragments with atomic number $6 \leq Z \leq 28$ measured in the $^{78}\text{Kr}+^{40}\text{Ca}$ reaction.

EXPERIMENTAL RESULTS

The experiment was carried out at the GANIL facility. Beams of $^{78,82}\text{Kr}$ were accelerated to 5.5 MeV/A and impinged on a self-supported 1mg/cm² thick ^{40}Ca target. The kinetic energy and atomic number of the ejectiles were measured with the 4 π -INDRA array [1]. Here, we report on characteristics of charged products emitted in the $3 \leq \theta_{lab} \leq 45$. For this angular domain, each detection ensemble is made of three layers: ionization chamber, silicon detector and CsI. The energy calibration was obtained from elastic scattering with beams of various q/A selected with the CIME cyclotron.

Kinematic features of the emitted fragments provide important clues about the reaction mechanisms. The centre-of-mass average velocity V_{cm} and the angular distributions for fragments with atomic number $Z=10, 15, 20, 25$ are shown in fig.1 for the $^{78}\text{Kr}+^{40}\text{Ca}$ reaction. The average centre-of-mass velocity V_{cm} for each Z -species are shown in fig.1c. To extract the velocity, the average mass of a given fragment is deduced from its atomic number using an empirical formula [2]. The centre-of-mass average velocity V_{cm} is roughly independent of the emission angle and agrees with the predictions deduced from the Viola systematic [3] (horizontal lines in fig.1a). These features suggest a strong degree of relaxation in the formation mechanism of the observed fragments and an emission governed mainly by Coulomb interaction. The Coulomb origin is also supported by the quasi-linear decrease of $\langle V_{cm} \rangle$ with increasing fragment Z -value (fig.1c). The angular distributions $d\sigma/d\theta_{cm}$ are rather flat (fig.1b) as in a case of fission from compound nuclei with large angular momentum. These characteristics are consistent with an emission from a compound nucleus (CN). Similar results are obtained for the $^{82}\text{Kr}+^{40}\text{Ca}$ reaction. The absolute cross-sections were deduced from the normalization with respect to the elastic scattering measured at a laboratory angle for which the cross-section is given by the Rutherford scattering.

The measured charge distributions are shown in fig.2a for the $^{78}\text{Kr}+^{40}\text{Ca}$ reaction (open circle). The cross-section distributions present a shape with a maximum around $Z=28$ which corresponds to half of the charge of the CN. This indicates that elements with $Z \geq 14$ come mainly from a symmetric fission process (see also fig.3b). For frag-

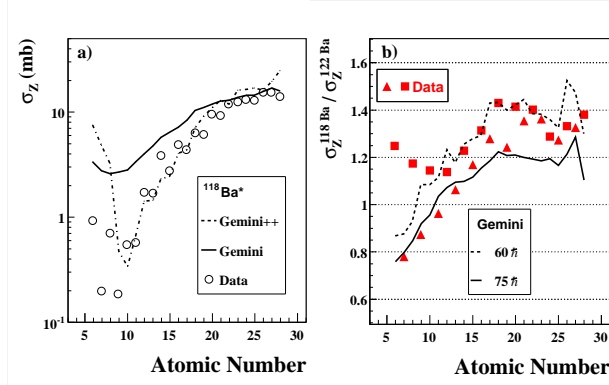


FIGURE 2. a) Experimental cross sections for fragments emitted in the $^{78}\text{Kr}+^{40}\text{Ca}$ reaction (open circles), compared to GEMINI (broken line) and GEMINI++ (dashed line) predictions assuming $J_{max}=65\hbar$; b) Experimental ratio $\sigma_Z^{118\text{Ba}}/\sigma_Z^{122\text{Ba}}$ for odd-Z fragments (triangles) and even-Z fragments (squares) compared to GEMINI calculations for $J_{max}=60\hbar$ (dashed line) and $J_{max}=75\hbar$ (broken line)

ments with $Z \leq 10$ a strong odd-even staggering is visible, and this effect is still present for higher Z with a smaller amplitude. Similar features are observed for the $^{82}\text{Kr}+^{40}\text{Ca}$ reaction, but the yields around the symmetric splitting are about 30% smaller than for the $^{78}\text{Kr}+^{40}\text{Ca}$ system. A probable explanation would be that the fission barrier for the neutron poor CN is smaller than for the neutron rich one. Since the cross-section depends on the thermal energy left once the collective energy is subtracted, a higher cross-section is expected for symmetric fission of the ^{118}Ba CN. The cross-sections for odd-Z fragments are higher for the neutron rich CN while cross-sections for even-Z fragments are higher for the neutron poor CN. To quantify this effect, the Z -dependence of the ratio $R = \sigma_Z^{118\text{Ba}} / \sigma_Z^{122\text{Ba}}$ is reported on fig.2b. R decreases roughly from 1.25 for $Z=6$ down to 0.75 for $Z=7$. For odd-Z (triangles), the ratio increases up to $Z=21$ and reaches a kind of plateau. For even-Z (squares), R decreases from $Z=6$ to $Z=10$ and then increases to reach the same kind of plateau as for odd-Z. The excitation energy and the maximum angular momentum stored in the compound nucleus are expected to be very similar in both reactions. Thus, the observed effects are probably linked to the difference in the (N/Z) of the CN. To summarize, we observe the coexistence of features that reasonably reflect the role of the angular momentum, and a staggering behaviour which reflects the persistence of structure effects in the process, or/and the influence of the secondary decays. In the next section we discuss these aspects in the framework of a statistical approach.

COMPARISON WITH STATISTICAL APPROACH

Statistical decay calculations were performed using the GEMINI [4] code. All decay channels are calculated within the Hauser-Feshbach model for $Z \leq 2$ and transition state formalism of Moretto for $Z \geq 3$. The key ingredient to describe the fragment emission is the conditional saddle configuration. The saddle conditional energy for different mass (or charge) asymmetry was deduced from the rotating finite-range model developed by Sierk [5]. More details can be found in [4].

The fusion cross-section comprises the fusion-evaporation and fusion-fission components. In this work, the fusion evaporation cross-section is not yet available. However, the fission cross-section is sensitive to the highest angular momentum leading to fission. The maximum angular momentum J_{max} which reproduces the yields around the symmetric fission could be considered as a good estimate of the J_{max} for fusion. Thus, calculations were performed assuming a CN spin distribution given by the sharp cut-off approximation with the value of J_{max} taken as a parameter.

The shape of the charge distribution around the symmetric fission could be satisfactorily reproduced by varying J_{max} and the level density parameter values in a reasonable range for these reactions at low excitation energies (J_{max} between $60\hbar$ and $75\hbar$ and a level density parameter value between $a=A/8$ and $a=A/9$). In fig.2a are shown the predictions for the disintegration of a ^{118}Ba assuming $J_{max} = 65\hbar$ and $a=A/8.5$. The model reproduces well the charge distribution around the symmetry. However, the yields for light fragment emission are overestimated by the model. The yields for light fragments are well reproduced assuming $J_{max} = 50\hbar$ but the yields at symmetry are underestimated by almost a factor 10 (not shown). These disagreements would indicate a failure of the Sierk barriers and/or the transition state picture at large mass (charge) asymmetry and large angular momentum. Predicted values of the ratio $\sigma_Z^{118\text{Ba}} / \sigma_Z^{122\text{Ba}}$ are shown in fig.2b for two values of J_{max} ($60\hbar$ (dashed line) and $75\hbar$ (broken line)). The calculations reproduce qualitatively the experimental data for light fragments with odd-Z and for $Z \geq 14$ but strongly underestimates the yields of light even-Z fragments.

In this analysis we have used the sharp cut-off approximation at variance with models which predict a diffuse distribution for the angular momenta leading to fusion. However, a finite value of the diffuseness would not change drastically the predicted relative yields between light fragment emission and symmetric fission, and would not explain the specific behaviour of the ratio R for $Z \leq 14$.

The persistence of staggering effects would seem to indicate that light fragments could be emitted relatively cold or at a later stage of the separation process. Coincidence data between light particles and fragments bring more insights on the emission process, as will be presented in the following.

COINCIDENCE DATA

All light charged particles and fragments emitted in the angular range $3 \leq \theta_{lab} \leq 45$ are included in the following event-by-event analysis. In order to study only products coming from the disintegration of a CN, events with a total measured charge greater than 48 have been considered.

The correlation between the two biggest fragments Z_1 and Z_2 is shown in fig.3a for the $^{78}\text{Kr}+^{40}\text{Ca}$ reaction. Data are not corrected for efficiency. In the correlation plot, the two maxima in the yields correspond to fission and evaporation components. The ridge is slightly shifted to an average value smaller than the charge of the CN ($Z=56$), which reflects a weak light charged-particle emission. The Z distribution for the $^{78}\text{Kr}+^{40}\text{Ca}$ reaction (fig.3b) indicates both fission-fragments and residues components. It is worth noting that the relative yield between fusion-fission and fusion-evaporation processes is biased due to the criterion on total measured charge in the limited angular range.

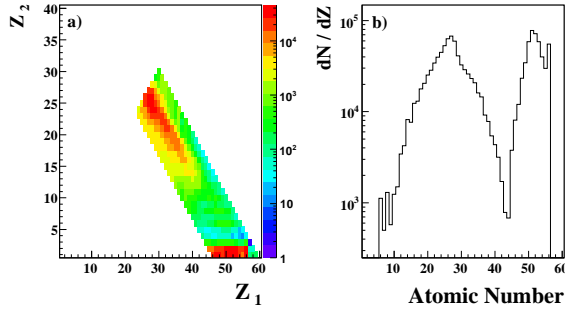


FIGURE 3. Correlation between the two biggest fragments Z_1 and Z_2 (a) and Z distribution (b) for the $^{78}\text{Kr}+^{40}\text{Ca}$ reaction.

In fig.4 are shown the kinetic energy distributions of $Z=2$ particles emitted in coincidence with fragments of different sizes, from evaporation residues (top left panel) to the symmetric splitting (bottom right panel). All spectra have been arbitrarily normalised to unity to discuss the shape evolution of the energy distribution. Looking at the two extremes of charge asymmetry, we can see spectra with a single component for particles emitted in coincidence with residues, while particles emitted during the fission process are characterised by spectra with two components. For emission particles in coincidence with the residues, the shape of the kinetic energy distribution is akin to an evaporation spectrum from a hot CN. In the symmetric splitting case, the high kinetic energy component of the energy spectra could be attributed to an emission from a system evolving from the saddle to the scission configuration, while the low kinetic energy component would be associated to the emission from fragments after separation. The same feature is also observed on a broad range of charge asymmetry as indicated in the three bottom panels of fig.4. Interestingly, the location of the peak and the slope of the high kinetic energy component are similar for the range $16 \leq Z \leq 40$ (e.g the fission peak) which suggest that particles are emitted from an intermediate system having equivalent properties in shape and temperature while the final states are very different. This is at variance with the results obtained in [6] showing an increase of the interaction barrier of about 5 MeV from $Z=16$ to $Z=40$. Finally, for asymmetric splitting, the component at high kinetic energy is still observed. Moreover, this component dominates the full spectrum which indicates a weak post-scission emission of light charged particles. Consequently, the odd-even staggering effect observed in the yields of light fragments could be reasonably due to the low excitation energy left at the scission stage, otherwise the staggering would have been blurred by the disintegration process. These features have been deduced from the integrated kinetic energy spectra measured in a limited angular range since data have not yet been fully reduced. Thus it is premature to extract the pre-scission and post-scission light particles properties by using an appropriate procedure as, for example, the well-known multiple-sources method. This kind of analysis will be performed in a near future.

These experimental characteristics call for a dynamical description of the evolution of a system on a potential energy surface including structure effects sensitive to the neutron enrichment of the emitting CN. This is challenging for models. In this work,

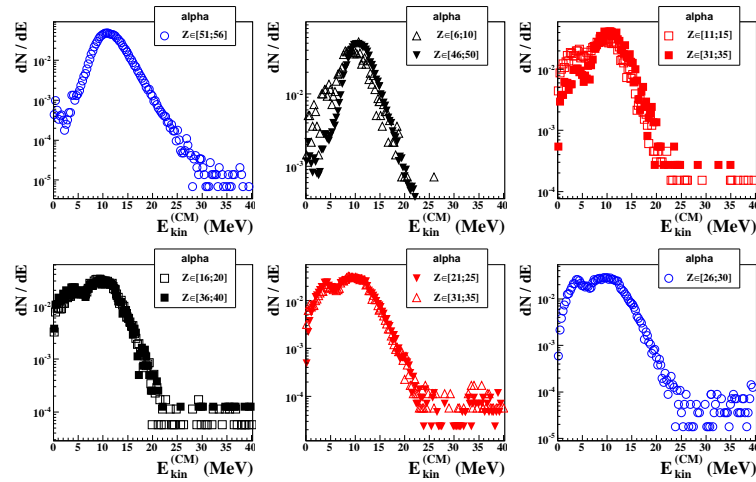


FIGURE 4. Kinetic energy distributions of $Z=2$ particles emitted in coincidence with fragments. Gates on the Z values are indicated in each panel. See text.

we have used an approach proposed in [7] (GEMINI++). The code is based on both pre-fission neutron emission data [8] and widths of fragment distributions in the fission process [9]. The temperature at the saddle configuration is deduced from the energy removed by the pre-fission emission and the width of the fission fragment distribution is deduced from [9] which links the temperature at saddle configuration and the width of the fragment distribution. Results of the calculation are presented in fig.2a (dashed line) for the $^{78}\text{Kr}+^{40}\text{Ca}$ reaction assuming $J_{max} = 65\hbar$ and $a=A/8.5$. The predicted cross-sections agree very well with the experimental data except for fragments with atomic number $Z=6,7,8$ for which no data are available in [9]. Even though more quantitative analysis is required, the agreement with the experimental data support a scenario of pre-fission light charged particle emission in the mechanism of the fragment formation produced in the $^{78}\text{Kr}+^{40}\text{Ca}$ reaction at 5.5 MeV/A. Further investigations are foreseen to explore quantitatively the influence of the N/Z ratio on the pre-fission and post-fission light charged particles emission process.

REFERENCES

1. J. Pouthas *et al.*, *Nucl. Instrum. Methods Phys. Res.* **A357**, (1995), 418.
2. R.J. Charity *et al.*, *Nucl. Phys.* **A476**, (1988), 516.
3. C. Beck *et al.*, *Phys. Rev.* **C53**, (1996), 1989.
4. R.J. Charity *et al.*, *Nucl. Phys.* **A483**, (1988), 43.
5. A.J. Sierk, *Phys. Rev.* **C33**, (1986), 2039.
6. W.J. Parker *et al.*, *Phys. Rev.* **C44**, (1991), 774.
7. R.J. Charity, code GEMINI++(www.chemistry.wustl.edu/rc/gemini++/).
8. D. Hinde *et al.*, *Phys. Rev.* **C45**, (1992), 1229.
9. Y. Rusanov *et al.*, *Phys. At. Nucl.* **60**, (1997), 683.